BENCHMARKING STEPWISE RAY-TRACING IN RINGS IN PRESENCE OF RADIATION DAMPING*

F. Méot

Collider-Accelerator Department, BNL, Upton, NY 11973, USA.

Abstract

A number of machine design studies, including "nano-beams", sub-millimeter "beta*" optics, SR rings, etc., require high accuracy on beam orbit and beam size, reliable evaluation of machine parameters, dynamic apertures, etc. This can only be achieved using high precision simulation tools. Stepwise ray-tracing methods belong in this category of tools, stochastic synchrotron radiation and its effects on an electron beam in a storage ring are simulated here in that manner. Benchmarking of the method against analytical model expectations, using a Chasman-Green cell, is presented.

INTRODUCTION

Several present accelerator, storage rings or collider projects involve extremely low emittance lepton beams, their design requires high accuracy on beam orbit and beam size, reliable evaluation of machine parameters, dynamic apertures, etc. This can only be achieved using high precision simulation tools, not only based on reliable integration techniques, but also involving a correct representation of the forces (magnetic and/or electric fields). For that reason potentialities of stepwise ray-tracing methods in that matter have been checked and benchmarked against analytical model expectations, in a synchrotron radiation (SR) storage ring using a Chasman-Green cell [?].
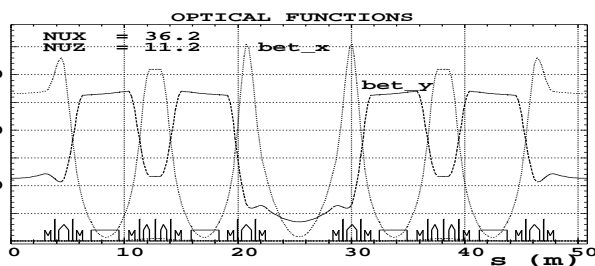

Figure 1: Optical functions in the Chasman-Green super-cell.

The ray-tracing code Zgoubi [?] is used in that exercise. Stochastic synchrotron radiation (SR) in beam lines was introduced in Zgoubi in view of assessing its perturbing effects on beam emittance in the beam delivery system of the "Linear Collider" [?]. The method for handling

stochastic SR closely followed from earlier works regarding the DYNAC dynamics code developed at Saclay [?] in designing recirculating arcs in the ELFE project [?]. These numerical tools have recently been applied successfully in rings [?].

Note that, although not addressed here and yet part of the motivations for the work, it is further planned to develop the method so to include SR effects on spin dynamics in complement to existing spin machinery [?], namely via spin diffusion and Sokholov-Ternov polarization, in view of possible application in design studies as the e-p collider [?].

WORKING CONDITIONS

Lattice The benchmarking exercises discussed here use a Chasman-Green super-cell for the reason that many quantities relevant to beam dynamics under SR effects can be derived analytically in that case, as the chromatic invariant, equilibrium emittance, damping times, etc. The considered cell is a variant of ESRF one, a storage ring is built from 16 such cells, storage energy ranges from 6 GeV to 18 GeV (convenient to our demonstration, if not realistic) depending on the "numerical experiment" of concern.

Tab. **??** gives the general lattice parameters, the optical functions are displayed in Fig. **??**.

RF Assuming for benchmarking purposes an isomagnetic lattice, SR losses amount to

$$U_s = \frac{C_\gamma}{2\pi} E_s^4 I_2 \overset{iso-\rho}{=} C_\gamma \frac{E_s^4}{\rho} \approx 4.6 \text{ MeV/turn}$$

restored by the RF system. A single cavity is considered for simplicity, with somewhat arbitrary parameters, bottom of Tab. **??**, including 30 degrees synchronous phase resulting in a peak voltage twice the energy loss.

RAY-TRACING RESULTS

The sole effect of energy loss is accounted for in the numerical ray-tracing, although Zgoubi allows accounting for momentum kick. In addition, SR in sole bends is considered (no radiation in quadrupoles nor sextupoles), so to allow relevant comparison with numerical values drawn from SR theory.

Typical data from which damping parameters are drawn are displayed in Fig. **??**.

Beam Dynamics and EM Fields

Table 1: Chasman-Green Lattice Parameters, Notations Used in the Text

|		
Cell length	(m)	50.8000
Number of cells		16
Circumference, $\mathcal{C} = 2\pi R$	(m)	812.800
momentum compaction, α	(10^{-4})	3.096
Qx		36.1998
Qy		11.1997
Q'x, Q'y, natural		-113.9, -34.53
Q'x, Q'y, corrected		-0.035, -0.012
Bend parameters:		
Nb. of bends		64
Bend deviation, θ	(rad)	$2\pi/64$
Bend length, $\mathcal{L}$	(m)	2.45
Curvature radius, ρ	(m)	24.95549
Periodic functions at non-dispersive dipole end:		
β_0	(m)	3.415
α_0		2.073
Longitudinal parameters:		
Frequency, $f_{rf} = \omega_{rf}/2\pi$	(MHz)	110.651
Harmonic, h		300
Synchronous phase, φ_s	(deg)	30
Peak voltage, $\hat{V}$	(MV)	9.1912
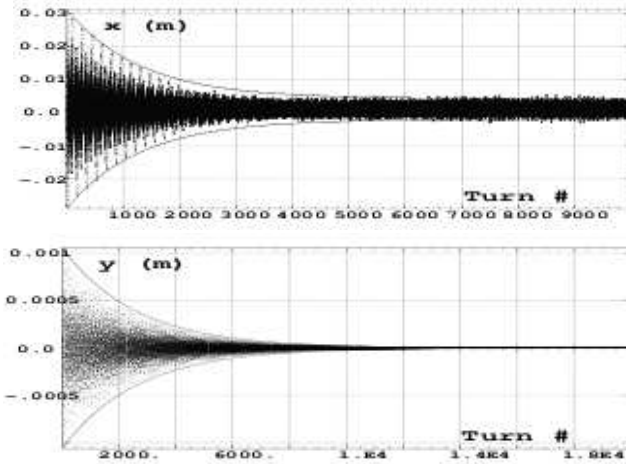
Figure 2: Transverse damping, samples. Top: horizontal motion, down to equilibrium emittance ; bottom: vertical, down to zero (since no transverse kick is accounted for). The envelopes (solid lines) are from the damping law with numerical parameters as given in Tab. **??**.

SR integrals intervene in the various quantities object of benchmarking in Tab. **??**. Their numerical values as drawn from respectively theoretical expressions and ray-tracing are given in Tab. **??**. Note that ray-tracing does not directly provide $I_1 - I_5$ values, these are drawn from the damping effects and their parameters instead, like damp-

Table 2: SR Integrals and their Reduced Expressions for Isomagnetic Lattice

		Theoretical	Ray-tracing
$I_1^{(a)} = \alpha\mathcal{C}$	(m)	0.2516	0.250 [c]
$I_2 = 2\pi/\rho$	(m^{-1})	0.2518	0.253 [d]
$I_3 = 2\pi/\rho^2$	(10^{-2}m^{-2})	1.0089	0.102 [e]
$I_4 = \frac{1}{\rho^3}\int D_x ds$	(10^{-4}m^{-1})	4.0403	– [f]
$I_5 = \frac{2\pi}{\rho^2}\bar{\mathcal{H}}$ [b]	(10^{-5}m^{-1})	3.2562	3.21 [g]
$\bar{\mathcal{H}}$	(mm)	3.2209	3.207 [h]
$\bar{\mathcal{H}}_{min} = \frac{\rho\theta^3}{4\sqrt{15}}$	(mm)	1.5242	

(a) $I_1 = \int \frac{D_x}{\rho} ds$, $I_2 = \int \frac{ds}{\rho^2}$, $I_3 = \int \frac{ds}{|\rho|^3}$, $I_4 = \int \frac{D_x}{\rho^3}(1-2n)\,ds$, $I_5 = \int \frac{\mathcal{H}}{|\rho|^3} ds$, $\bar{\mathcal{H}} = \frac{1}{2\pi\rho}\int_{bends} \mathcal{H}ds$, with, in I_4, $n = -\frac{\rho}{B}\frac{\partial B}{\partial x}$ =field index= 0.

(b) $\mathcal{H} = \gamma_x D_x^2 + 2\alpha_x D_x D_x' + \beta_x D_x'^2 \overset{(CG)}{=} \rho\theta^3(\frac{\gamma_0\mathcal{L}}{20} + \frac{\beta_0}{3\mathcal{L}} - \frac{\alpha_0}{4})$ case of Chasman-Green cell, α_0, β_0 from Tab. **??**, $\gamma_0 = (1+\alpha_0^2)/\beta_0$.

(c) From momentum compaction.

(d) From energy loss, U_s, Tab. **??**.

(e) $I_2^2/(2\pi)$.

(f) From I_4/I_2, damping parameter $\mathcal{D}$, Tab. **??**.

(g) From I_5/I_2, natural ϵ_x, Tab. **??**.

(h) From natural ϵ_x, Tab. **??**.

ing times, momentum spread, bunch length, etc.: this is detailed in footnotes in Tab. **??**.

Damping times, equilibrium emittances, bunch sizes, etc., so drawn from ray-tracing are displayed in Tab. **??**. together with theoretical data for comparison, it can be observed that the agreement is very good.

Theoretical exponential damping laws for four different energies, 6, 9, 12 and 18 GeV, are plotted in Fig. **??** (longitudinal motiuon) and Fig. **??** (horizontal) together with a fitting curve using $\epsilon(t) = \epsilon_0 \exp(-t/\tau) + \epsilon_f$ with τ the damping time constant, ϵ_0 and ϵ_f respectively the starting and equilibrium emittances. Numerical values for τ, ϵ_0 and ϵ_f as obtained from the fit are given in Tab. **??**, together with the theoretical ones (as drawn from the formulæ given in Tab. **??**) for comparison.

Scaling laws with energy for various quantities in Tab. **??** are checked. Tab. **??** shows the numerical values of emittances and damping times as drawn from smoothing of ray-tracing data using the exponential damping fit above. The Table shows, for comparison, *between square brackets*, numerical values drawn from theoretical formulæ in Tab. **??**.

CONCLUSION

Ray-tracing reproduces very accurately beam parameters associated with synchrotron radiation damping. That makes the method a relevant tool in design studies regarding nanobeams, resonance factories and other e-p collider projects.

Table 3: Synchrotron Radiation Parameters at 6 GeV. The "Theoretical" Column Shows Both the Formula Used and the Numerical Value It Yields.

		Zgoubi	Theor.
Working hypotheses:			
Storage energy, E_s	GeV		6
γ			11742
Revolution period T_{rev}	μs		2.7112
Lattice parameters:			
Damping parameter, $\mathcal{D}$	10^{-3}		1.6049 I_4/I_2
J_x		$1.0262^{(b)}$	0.9984 $1-\mathcal{D}$
J_y		$0.9832^{(c)}$	1
J_l		$2.0044^{(d)}$	2.0016 $2+\mathcal{D}$
$J_x+J_y+J_l$		4.01	4
Energy relevant parameters:			
Energy loss/turn, U_s	MeV	$4.616^{(a)}$	4.594 $\frac{\mathcal{C}_\gamma}{2\pi}E_s^4 I_2$
Critical energy, u_c	keV	$19.20^{(a)}$	19.20 $\frac{3\bar{h}\gamma^3 c}{2e\rho}$
Photons per turn		$776.5^{(a)}$	777.1 $\frac{15\sqrt{3}U_s}{8u_c}$
Natural rms emittances:			
horizontal, ϵ_x	nm	$6.80^{(g)}$	6.829 $\frac{\mathcal{C}_q\gamma^2}{J_x}\frac{I_5}{I_2}$
minimal ϵ_x, $\epsilon_{x,min}$	nm		3.232 $\frac{\mathcal{C}_q\gamma^2}{J_x}\frac{\theta^3}{4\sqrt{15}}$
longitudinal, ϵ_l	μeV.s	$22.2^{(g)}$	22.18 $\sigma_\varphi\,\sigma_{\frac{dE}{E}}$
rms dE/E, $\sigma_{\frac{dE}{E}}$	10^{-3}	$1.023^{(g)}$	1.028 $\sqrt{\frac{\mathcal{C}_q}{J_l\rho}}\gamma$
rms bunch length	mm	$9.40^{(g)}$	9.301 $\frac{\alpha c}{\Omega_s}\sigma_{\frac{dE}{E}}$
Damping times:			
horizontal, τ_{ϵ_x}	ms	$3.432^{(g')}$	3.547 $\frac{T_{rev}E_s}{U_s J_x}$
	turns	1266	1308
vertical, τ_{ϵ_y}	ms	$3.582^{(g')}$	3.541 $\frac{T_{rev}E_s}{U_s J_y}$
	turns	1321	1306
longitudinal, τ_{ϵ_l}	ms	$1.757^{(g')}$	1.769 $\frac{T_{rev}E_s}{U_s J_l}$
	turns	648	652

(a) Statistical, from tracking.
(b) From τ_{ϵ_x} value.
(c) From τ_{ϵ_y} value.
(d) From $\sigma_{\frac{dE}{E}}$ or τ_{ϵ_l} values.
(e) Dipoles have zero field gradient.
(g) From tracking, 1000 particles.
(g') Given (g), with $\epsilon(t)=\epsilon_{initial}\,e^{-t/\tau}+\epsilon_{equil.}$.
(h) $\mathcal{C}_\gamma=\frac{4\pi}{3}\frac{r_e}{(m_ec^2)^3}\approx 8.846276\,10^{-5}$[m/GeV^3].
(i) $\mathcal{C}_q=\frac{55}{32\sqrt{3}}\frac{\bar{h}}{m_ec}\approx 3.831938\,10^{-13}$[m].
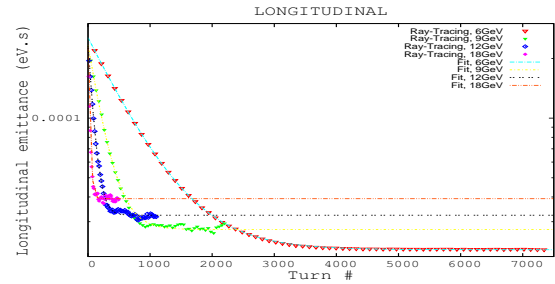

Figure 3: Damping of longitudinal motion, 6, 9, 12 and 18 GeV.

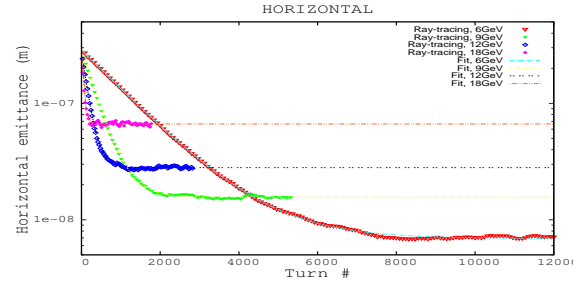

Figure 4: Damping of horizontal motion, 6, 9, 12 and 18 GeV.

Table 4: Scaling With Energy. Expected γ- and θ-Dependence Is Recalled in the 3rd Row, Energy Loss is Recalled in the 2nd Column. Theoretical Values in [].

	Energy loss, U_s (MeV)	ϵ_l (eV.s)	τ_l (ms)	ϵ_x (nm)	τ_x (ms)
Scaling law	$\gamma^4\,\theta$	$\gamma^{1/2}\theta$	$1/\gamma^3\theta$	$\gamma^2\,\theta^3$	$1/\gamma^3\theta$
6 GeV	4.616 [4.594]	21.7 [22.18]	1.755 [1.7690]	6.92 [6.83]	3.422 [3.5466]
9 GeV	23.4 [23.257]	27.4 [27.17]	0.575 [0.5242]	15.6 [15.37]	1.016 [1.0508]
12 GeV	73.9 [73.505]	32.4 [31.37]	0.222 [0.2211]	28.0 [27.32]	0.447 [0.4433]
18 GeV	374 [372.121]	39.2 [38.42]	0.0676 [0.0655]	66.5 [61.46]	0.135 [0.1314]

REFERENCES

[1] http://en.wikipedia.org/wiki/Chasman-Green_lattice.

[2] The ray-tracing code Zgoubi, F. Méot, S. Valero, NIM A 427 (1999) 353-356. http://sourceforge.net/projects/zgoubi/

[3] Numerical tools for the simulation of synchrotron radiation loss and induced dynamical effects in high energy transport lines, F. Méot, J. Payet, int. rep. DAPNIA/SEA-00-01, CEA/DSM Saclay (July 2000).

[4] A new dynamics code DYNAC for electrons, protons and heavy ions in LINACS with long accelerating elements, P. Lapostolle, F. Méot, S. Valero, 1990 LINAC Conf., Albuquerque, NM, USA.

[5] Electron Lab for Europe, Blue Book, CNRS-IN2P3 (1994). SR perturbations in long transport lines, G. Leleux et al. IEEE 1991 Part Acc. Conf., San Francisco (May 1991).

[6] Lattice design tool developements regarding the super-B project, F. Méot, N. Monseu, Proc. IPAC 2010, Kyoto.

[7] A numerical method for combined spin tracking and ray tracing of charged particles, F. Méot, NIM A 313 (1992).

[8] High luminosity electron hadron collider eRHIC, V. Ptitsyn, these procs.

Beam Dynamics and EM Fields

Dynamics 05: Code Development and Simulation Techniques